Excitation processes in low pressure plasmas

Angelica Brolin

Lund Observatory
Lund University

2010-EXA47

Degree project of 15 higher education credits
September 2010

Lund Observatory
Box 43
SE-221 00 Lund
Sweden

Abstract

Spectral lines from mercury, barium and krypton were investigated to determine the excitation processes efficient in a low pressure plasma The light from a fluorescent light tube will be dispersed by a Czerny-Turner spectrograph and recorded by an ICCD camera. A matlab script was used to cut out the wanted spectral line and integrate the intensity from left to right up and down over the spectral lines. The excitation processes in Hg II takes place in two or more step processes, because of the high ionization limit of Hg I. In Hg I the energy levels are probably populated by direct electron collision. There is an optimal electrical discharge current, which will not wear out the electrodes. The rare gas behaved as expected, the intensity rises with the current until saturation.

Sammanfattning

Plasmor brukar kallas för det fjärde aggregationstillståndet. En gas som är helt eller delvis joniserad är ett plasma. På jorden förekommer plasmor naturligt enbart i blixten och i norrsken, i rymden finns de i stjärnvindar, solflarer, stjärnatmosfärer, nebulosor och i det interstellära mediet. I det här arbetet undersöktes emissionslinjer från kvicksilver, barium och krypton för att fastställa vilka excitationsprocesser som är verksamma i lågtrycksplasmor.

En Czerny-Turner spektrograf och en ICCD-kamera användes huvudsakligen till att undersöka spektrallinjerna. Ljuskällan var ett 18 w lysrör producerat av Aura light. I neutralt kvicksilver besätts energinivåerna genom direkt elektronkollision. Excitationsprocesser som ger en-gång joniserat kvicksilver sker troligast i två eller fler-stegs processer på grund av den höga jonisationsgränsen hos neutralt kvicksilver. Mängden kvicksilver i lysröret ändras med temperaturen. Vid låga temperaturer minskar mängden kvicksilver. Det finns en ideal urladdningsström och temperatur för elektroden. Vid låga strömmar är elektroden kall vilket ger hög bariumemission, vid höga strömmar blir elektroden varm vilket medför förångning av barium. Detta är ett stort problem vid ’’dimning’’ av lysrör. Målet är att hålla temperaturen konstant även om urladdningsströmmen ändras. Intensiteten hos krypton ökade med strömmen tills saturering infann sig. I framtiden är fortsatta mätningar intressanta för att hitta ett bra sätt att dimma lysrören på, hitta bra gasblandningar och för att hålla ljusintensiteten konstant på kalla platser.

Table of contents

1. Introduction

A partly or completely ionized gas is considered to be a plasma. Plasmas occur in space and on earth and have several important practical applications, such as etching, sterilization, welding as well as wide variety of plasma applications for lightening proposes

Plasma studies are important in astrophysics because plasmas are common in space and it is possible to see the forbidden inter combination lines in space plasmas. The purpose of this work is to investigate the excitation processes inside of a low pressure plasma, and from those measurements observe the behavior of mercury, barium and krypton. As a function of the discharge current and the surrounding temperature, it is also possible to determine the optimal electrical discharge currents which will not wear the electrodes and how the energy levels in mercury will be populated and in which phase of the alternate current cycle most emissions take place. It is the differences in intensity that shows which excitation processes might be efficient and so on. Earlier investigations of the optimal discharge current and time resolved measurements have been preformed see [6] and [7].

Optical spectral emission was used to investigate the spectra. It is a great advantage using optical spectral emission because it does not cause any disturbance inside the plasma, but those processes which do not emit light are not observable with this method. The equipment mainly used was a Czerny turner spectrograph, an ICCD camera and a fluorescent light tube.

2. Plasma theory

Plasmas are usually referred to as the fourth state of aggregation. A gas that is partly or completely ionized, electrically neutral as a whole and where the main interaction is determined by free charges is defined to be a plasma [2]. Usually it is neutral, because ionization processes creates the same amount of negative and positive particles and any imbalance between positive and negative charges tend to be counteracted by electrostatic forces. The only naturally occurring plasmas on earth are lightening and aurora, but space plasmas occur in nebulas, the interstellar medium, stellar winds, stellar atmospheres and solar flares. Plasmas can be created by heating a gas to a special point, a few thousand K, so the random kinetic energy of the molecules at least partly exceeds the ionization limit. To determine the state of an ordinary material at least three parameters have to be known, such as pressure, temperature and density, but in a plasma one have to determine more parameters, such as electron and ion densities for instance.

A convenient way of making measurements in a plasma is using optical emission spectroscopy. The advantage is that the plasma is not disturbed, but processes which do not emit light such as absorption and ionization cannot be observed [2][8].

3. Processes in plasmas

In a plasma there are a number of processes that can change the charge and/or the excitation state of the atoms. These processes can be divided into radiative and collisional.

3.1 Radiative processes

Excited levels in an atom/ion can be populated by photon absorption from lower lying levels, or from radiative decay from the higher levels. If a level is populated by transitions from higher lying levels, this level is said to be populated by cascades [7].

Absorption $A + h\nu \rightarrow A^*$

Spontaneous emission $A^* \rightarrow A + h\nu$

Stimulated emission $A^* + h\nu \rightarrow A + h\nu + h\nu$

A represent the atom or ion, and A^* an excited state of the atomic system. The energy of the photon ($h\nu$), which is emitted or absorbed corresponds to the energy difference between two atomic levels.
To each of these three processes, a transition probability is associated, the Einstein coefficients [7].

The probability of spontaneous emission, A_{ul} gives the probability that the atom will decay radiatively from an upper level u to a lower level l. If level l is the only level the atom can decay to, the inverse to the transition probability will be the mean time spent in the upper level u and it is referred to as the lifetime of the upper level (τ_u) [7].

$$\tau_u = \frac{1}{A_{ul}}$$

Most of the emission from low-temperature plasmas is due to electric dipole emission, often referred to as allowed transitions. The transition probabilities for these allowed transitions are in the range of 10^8 s^{-1} – 10^9 s^{-1} and corresponding lifetimes in the order of ns. For heavier elements, transitions which break some of the selection rules of L-S-coupling are frequently observed. Levels which are depopulated by such transitions may have lifetimes ranging from ns to several seconds. In most plasmas studied on earth, the possibility of observing such transitions is usually limited by the collision frequency so very thin plasmas are needed to observe the forbidden lines. Thin plasmas occur in space, but successful observations of highly forbidden transitions have also been performed in laboratories using storage rings and ion traps [7].

A radiative process leading to ionization is called photo ionization. It may occur if a photon has an energy that exceeds the ionization energy. In contrast to photo-excitation, this is a non-resonant process and the excess energy is carried away as kinetic energy of the ionized free electron [7].

Photo ionization $A^z + h\nu \rightarrow A^{z+1} + e^-$

The kinetic energy of the free electron will not be quantized. Any photon with energy equal to or exceeding the ionization energy can cause photo ionization.
If photo ionization takes place from an excited level, correspondingly less energy is needed [7].

There is an inverse process to photo ionization, called radiative recombination.
Radiative recombination occurs when an electron is captured by an ion, where the surplus energy of the electron will be emitted as radiation. The final state of the atom may be the ground state or an excited state, which subsequently may decay by spontaneous emission of a photon [7].

Radiative recombination $A^z + e^- \rightarrow A^{z-1} + h\nu$

or

$$A^z + e^- \rightarrow A^{(z-1)*} + h\nu_1$$
$$A^{(z+1)*} \rightarrow A^{(z-1)} + h\nu_2$$

3.2 Collisional processes

Collisions can occur between atomic systems or between atoms and electrons.

Elastic scattering $A + B \rightarrow A + B$

where A and B are atoms or ions of the same or different kind. The internal energies of the atoms will not change [7].

If a collision is inelastic it will give rise to a change of the internal energies of the atomic system. The process in which the kinetic energy of the colliding particle transfers into excitation energy is called collisional excitation or collision of the first kind [7].

Collisional excitation $A + B \rightarrow A^* + B$

When an excited particle collides with another particle in its ground state, the excitation energy can be transferred into kinetic energy or internal energy of the other particle. This process is called super- elastic collision or collision of the second kind [7].

Super- elastic collision $A^* + B \rightarrow A + B^*$

Other collisional processes are charge transfer and ionization. In both of these two processes electrons will be transferred between atoms. In case of charge transfer any excess energy may result in the target atom being left in an excited state [7] .

Charge transfer $A^{z_1} + B^{z_2} \rightarrow A^{z_1-1} + B^{z_2+1}$

Ionization $A^{z_1} + B^{z_2} \rightarrow A^{z_1+1} + B^{z_2} + e^-$

The penning effect is similar to charge transfer, but one of the elements has a populated long-lived metastable excited level. If such an atom collides with an atom of an element with an ionization potential lower than that of the metastable level of the first atom, energy can be transferred into ionization of the second atom [7] .

Penning effect $A^{z_1*} + B^{z_2} \rightarrow A^{z_1} + B^{z_2+1} + e^-$

Excitation processes in plasmas are usually a combination of the processes mentioned above. One of the main parts of this work is to characterize and separate one step processes from multi step processes [7].

4. Theory of fluorescent tubes

A fluorescent light tube is a glass tube filled with a buffer gas, metallic mercury (4-10 mg) and a fluorescent powder deposited on the inner surface. The buffer gas consists of rare gases and the fluorescent powder consists of a mixture of phosphorous and other elements. When light from the UV-region hits the fluorescent powder it will be converted into visual light.

Mercury emits light mostly in the UV region, where the strongest lines are the resonance lines with wavelengths of 185 nm 254 nm. No lines from the UV-region will escape the tube because of the transmission properties of glass. The strongest visible lines are those going down to the triplet $^3P^o\,(5d^{10}6s^2 - 5d^{10}6s(^2S)6p)$ 405 nm, 436 nm and 546 nm [5][6].

The average energy of the electrons is in the range 1 eV.

In each end of the tube there is an electrode which is supplying the current. The electrodes are made of tungsten filament coated with alkaline earth metals (calcium, barium and strontium). These metals are used because they have a low work function, which makes it easier for electrons to leave the cathode [5].

When an (AC) electric current is applied, the electrodes will switch between being anode and cathode, the potential difference between the electrodes will create an electric field. A free electron will follow the electric field towards the anode, while positive ions travel towards the cathode. In the negative glow the rate of ion production is much larger than in the positive column. Between the negative glow and the cathode surface there is a large potential drop called the cathode fall which usually ranges between 5 and 15V.

The anode does not emit any positive ions so the currents have to be carried by electrons. The potential difference between the plasma and the anode is called the anode fall, usually

between 1 and 10 V. Between the positive column and the negative glow there is a dark region (about a cm), called Faraday dark space [1] *see Figure* 4.1.

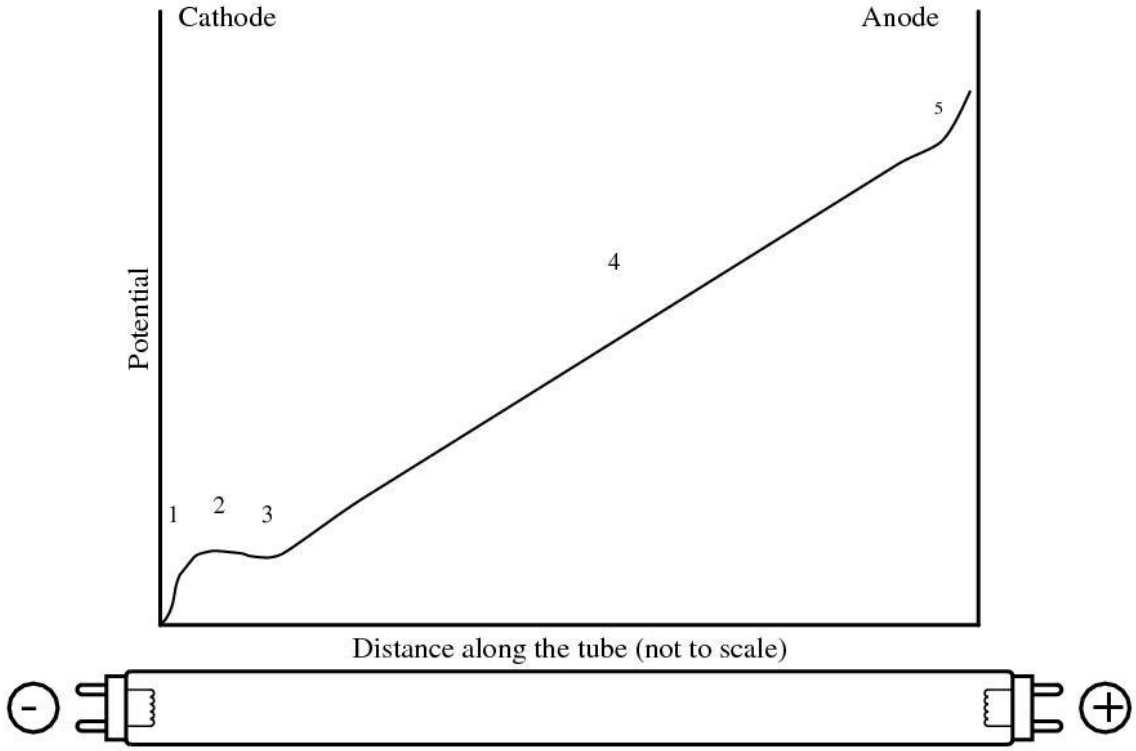

1. Cathode fall 2. Negative glow 3. Faraday dark space 4. Posivive column 5. Anode fall

Figure 4.1 shows the potential between anode and cathode in a fluorescent light tube.

5. Experimental setup

Two different setups were used in this diploma work. The difference between them is how the light source power was supplied *see Figure 6.5 and 6.6.*

5.1 Light source

The light source used was an 18 W T8 fluorescent light tube, provided by Aura light see *Figure 6.1*. The tube is partly covered with a homemade plastic cooling mantle. Near the electrodes the fluorescent powder has been removed in order to allow observation of the electrode region. Only the spectral lines from the visual region are accessible because of the transmission properties of glass. The buffer gas consisted of 15 % Argon and 85 % Krypon.

Figure 5.1 shows the light source.

5.2 Spectrograph

A 1 m Czerny-Turner grating spectrograph by Jarrel Ash with an ICCD detector system was used to record the spectra. The spectrograph has a 1200 lines/mm grating giving a reciprocal dispersion of about 8Å/mm in the first order, and a mechanical shutter controlled by the master PC trough the ANDOR iSTAR program package.

Light enters the first slit S_1 see *Figure 5.2* and then hits the mirror M_1 where it will be collimated and reflected. The parallel light will be dispersed by a plane grating G, and imaged by mirror M_2 onto the focal plane of the cooled (-20 ^{o} C) ICCD camera [3].
The camera is controlled from the computer program iSTAR. Information from the ICCD is sent to the iSTAR program; the spectra obtained will be saved as ascii files and subsequently loaded into matlab.

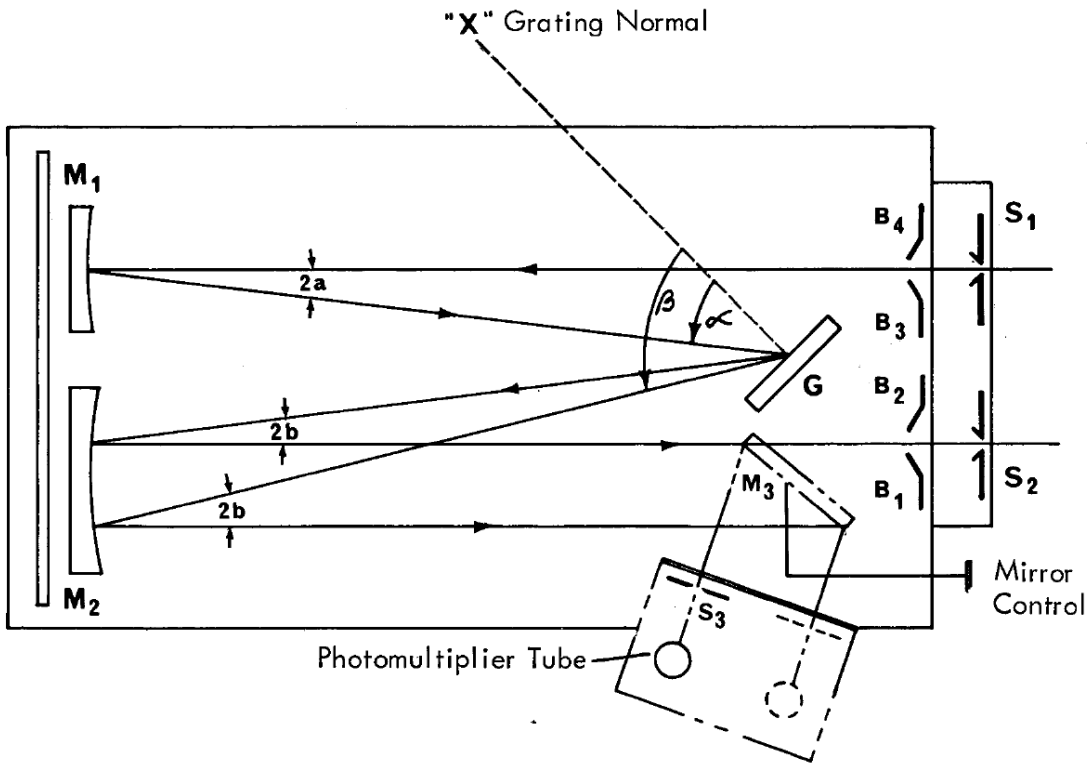

Figure 5.2 shows the shaping of the Czerny- Turner spectrograph.

5.3 ICCD (Intensified Charge-Coupled Device_) detector

The used detector is an Andor ICCD gateable detector model DH534-18H-03 FR, which is mounted onto the Czerny-Turner spectrograph [6] see *Figure 5.2.*

The ICCD detector has a gateable image amplifier which also work as an electric shutter with an on/off –time of 50 ns. It is thus possible to use the electric shutter to select light from any part of the alternate current cycle.

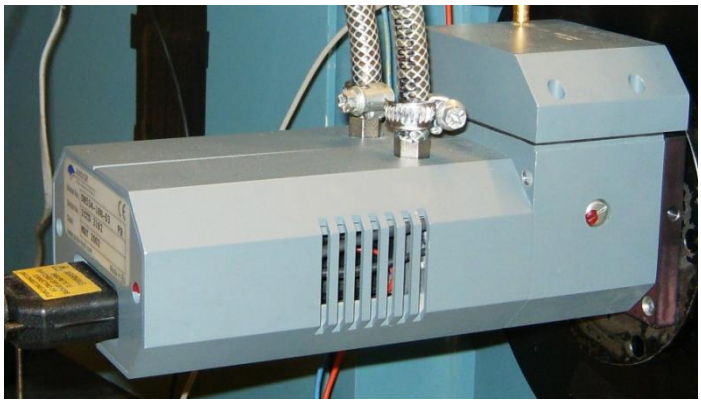

Figure 5.3 shows the ICCD detector.

5.4 Current probe

The discharge current is measured by a TCP202 15 Ampere AC/DC Current probe connected to a Tektronix oscilloscope with the TekProbe interface. The probe is suitable for measurements up to 15 A (DC + peak AC). On the head of the current probe there is a Hall Effect probe for measuring current, there is also a jaw which clamps on wires with a diameter of 3.8 mm or less. A Degauss-procedure removes residual magnetism from the probe core, which otherwise may cause errors in the measurements. A thumbwheel is used to compensate for smaller DC offsets of the probe output [4].

5.5 Microprocessor

The driving waveform and the gate control signals for the image intensifier are generated by microprocessor circuit, built around a Keil MCB 2100 prototype board equipped with a NXP LPC2129 ARM7 processor running at 60MHz, giving a time resolution of 17 ns. The waveform parameters and as the gate timing are controlled from a PC via a serial link. See *Figure 5.4 and 6.6.*

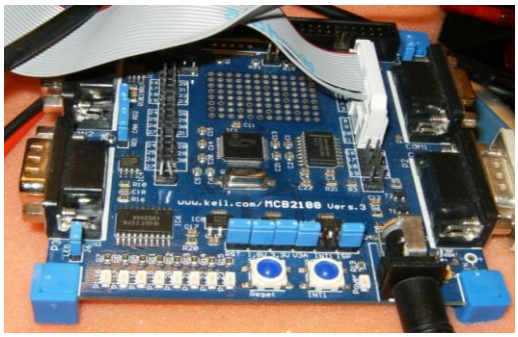

figure 5.4 shows the microprocessor.

5.6 Pump/cooling device

A pump (see *Figure 5.5)* will circulate water from a cooling device around the light tube to keep the temperature constant.

Figure 5.5 shows the circulating pump.

5.7 Andor iSTAR program

The spectra recorded by the ICCD are processed by a computer program called iSTAR from Andor technology Ltd. In this program you will be able to control parameters such as shutter time of the mechanical shutter, and the temperature of the ICCD detector.

5.8 Matlab program

A matlab script was used (*see appendix 12.2 A2 matlab script)* in this work. A 2-dimensional CCD image is loaded into the matlab program and normalized by division of the exposure time. The limits of the integration region and the background are determined by visual inspection of the image and the binned 1-dimensional spectrum *figure 5.6.* This gives the intensity of the chosen interval.

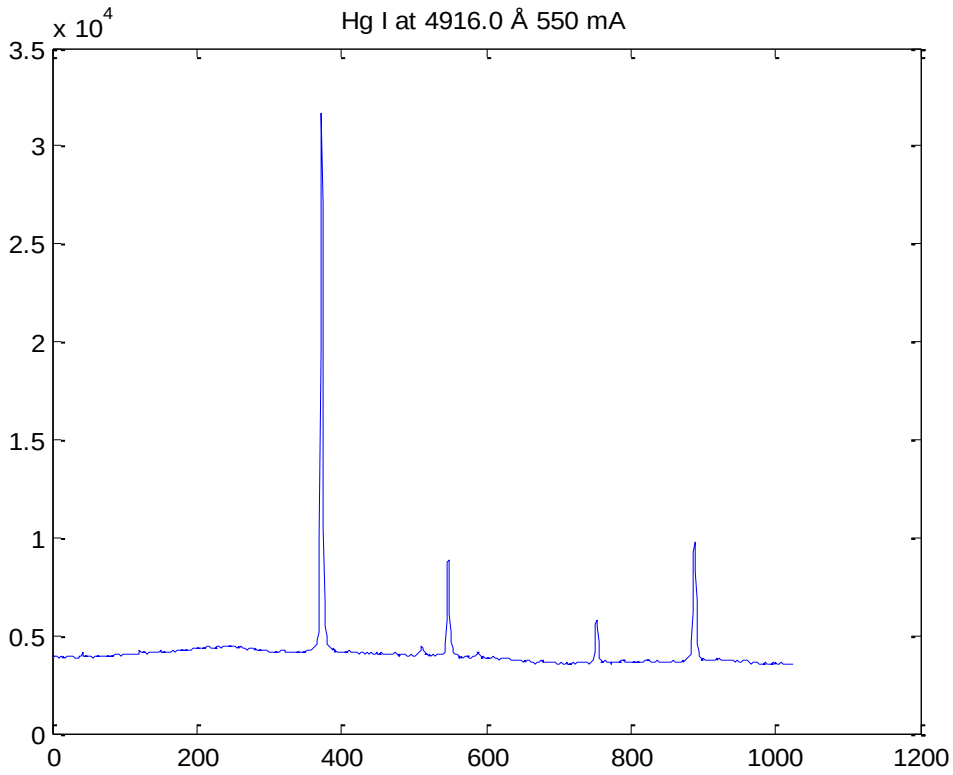

Figure 5.6 shows the spectrum of Hg I 4916.0 Å, the peak around 380 and 400 pixels is the one from Hg I. The integration limits of the emission peaks are found from the image.

6. Experiment

In this experiment four different spectral lines were investigated: Ba II 4554,0 Å, Hg I 4916,0 Å, Hg II 3983,9 Å and Kr I 4463,6 Å. The Hg I 4916,0 was chosen because many of the other Hg I lines are too strong, which makes them hard to handle experimentally. To investigate the strongest mercury lines, 4046 for example, the exposure time has to be of the same order as the cycle time and other means of attenuation therefore have to be used.

For the weak lines the exposure time is limited to 20 s due to noise buildup from the intensifier. The ICCD camera does not give any reasonable measurements for shutter times shorter than tens of a second.

Since there are no previous experiments of this kind to compare with, the spectral lines observed were selected mainly due to having a suitable intensity and falling into in an easily accessed wavelength range.

Table 6.1 observed transitions and the upper level energies relative to the ground state of the neutral atom

Element	Wavelength (Å)	Transition	Energies of the upper level (eV)
Hg II	3983,9	$5d^9 6s^2$-$5d^{10} 6p\ ^2D$-$^2P^o$	17.9
Kr I	4463,6	$4s^2 4p^5(^2P^o_{3/2})5s$-$4s^2 4p^5(^2p^o_{3/2})6p$	12.9
Ba II	4554,0	$6s$-$6p\ ^2S$-$^2P^o$	13.11
Hg I	4916,0	$5d^{10} 6s(^2S)6p$- $5d^{10} 6s(^2S)8s\ \ ^1P^o$-$^1S$	9,22

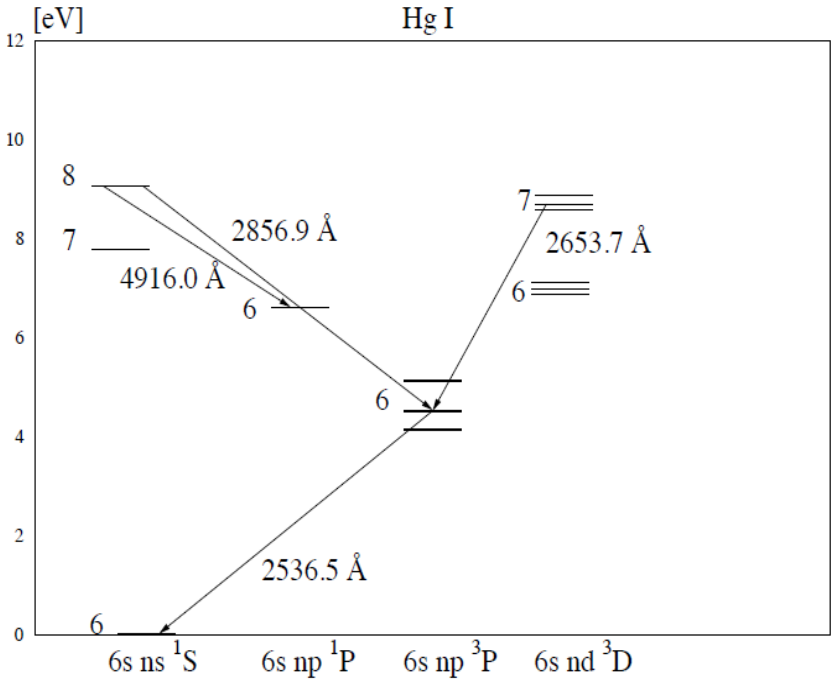

Figure 6.1 Energy level diagram showing the observed transition in Hg I.

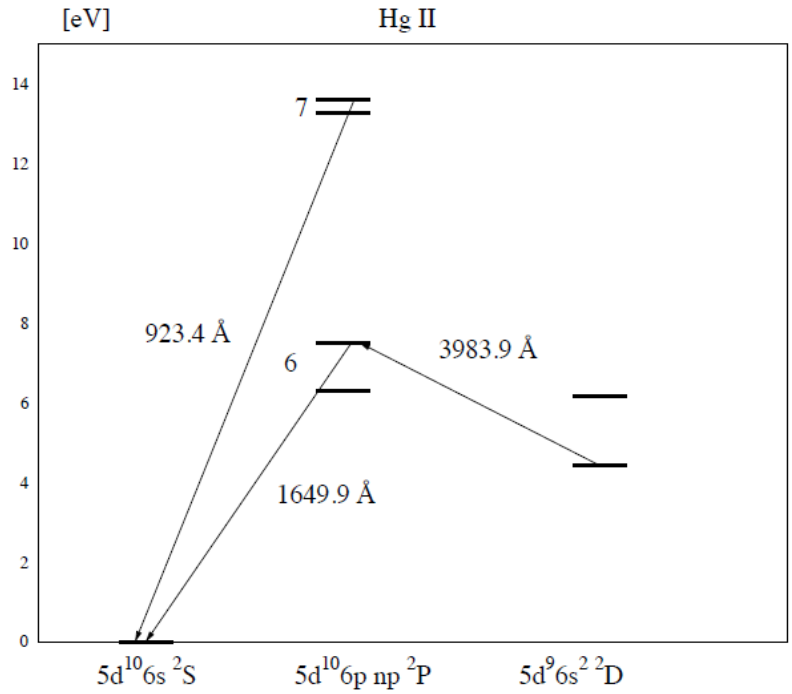

Figure 6.2 Energy level diagram showing the observed transition in Hg II.

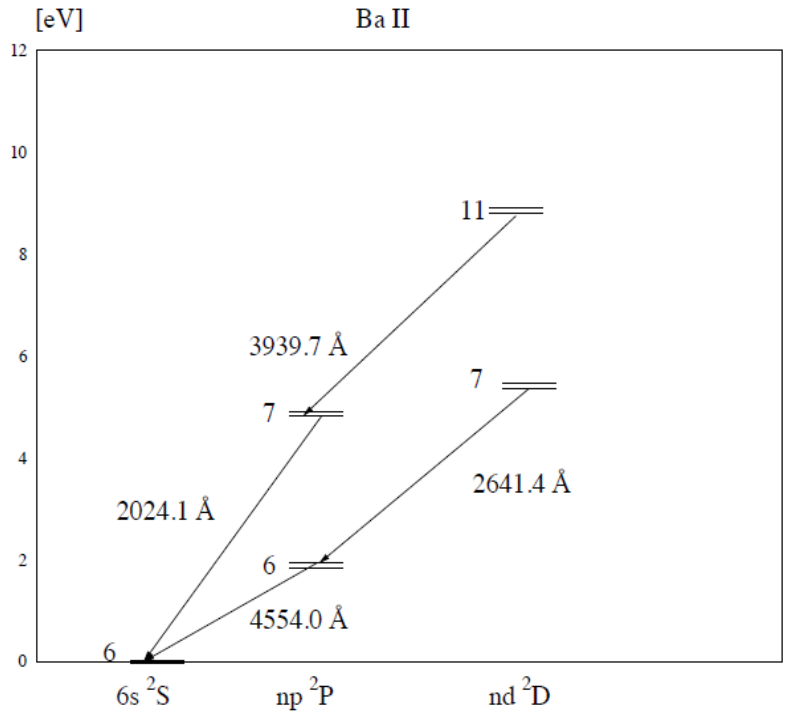

Figure 6.3 Energy level diagram showing the observed transition in Ba II.

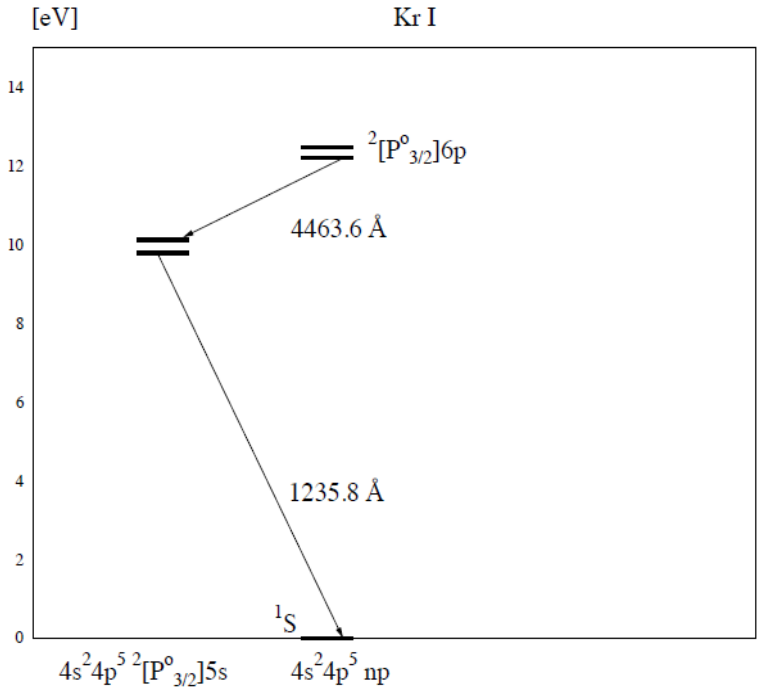

Figure 6.4 Energy level diagram showing the observed transition in Kr I.

Light from the fluorescent light tube is focused by a lens and dispersed by the Czerny-Turner grating spectrograph. There were some difficulties using this method. It was sometimes hard to determine how long the exposure time should be, if the spectral line was very weak or strong.
If the exposure time is two long the spectrum can be saturated in the ICCD detector. Sometimes it was hard to determine whether it was saturated or not. If the lines are saturated, the spectral line is smeared out and very strong; it is not possible to get any reasonable results from a saturated line.

The discharge current was varied between 150 mA and 850 mA in the first part of the experiment, in the second part it was varied between 100 mA and 500 mA. An oscilloscope Tekronix TDS 3034 and a current probe were used to set the currents.

During the experiment a pump was circulating water around the light tube to keep the temperature constant, otherwise the tube will be warmer at high currents and cooler at lower currents. Measurements were performed at T≈ 20° C and 0°C.

In the first part of the experiment the fluorescent light tube was powered by 50 Hz sinusoidal alternate current, the electrodes shifting being in anode and cathode phase all the time.

In the second part the gate generator makes it possible to separate the anode phase from the cathode phase and also to measure over any chosen interval of the AC cycle. Results from this experiment were very similar to the ones from the first part and confirmed that most of the emission takes place during the cathode phase.

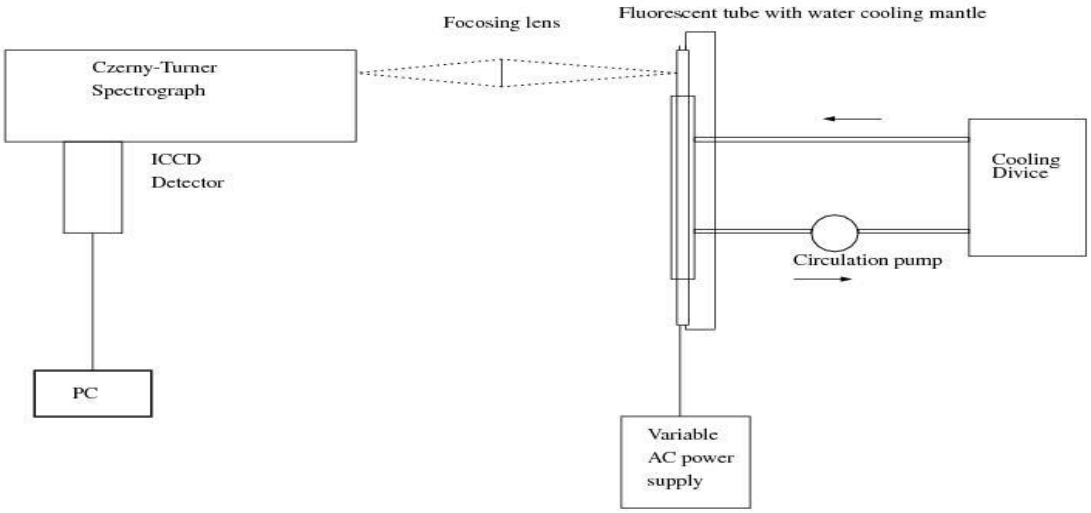

Figure 6.5 Shows the first experimental set up

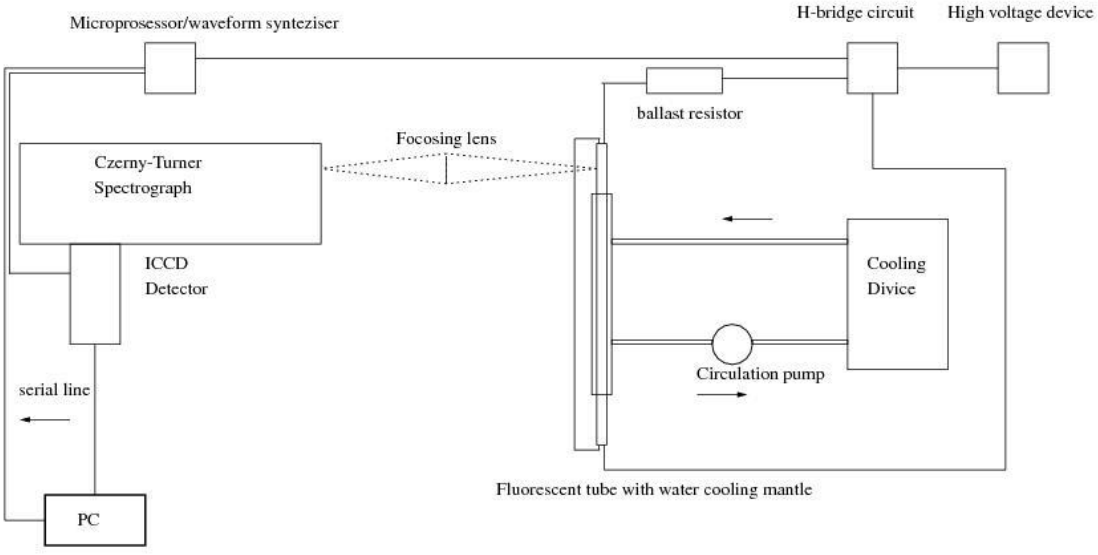

Figure 6.6 shows the second experimental set up

7. Result

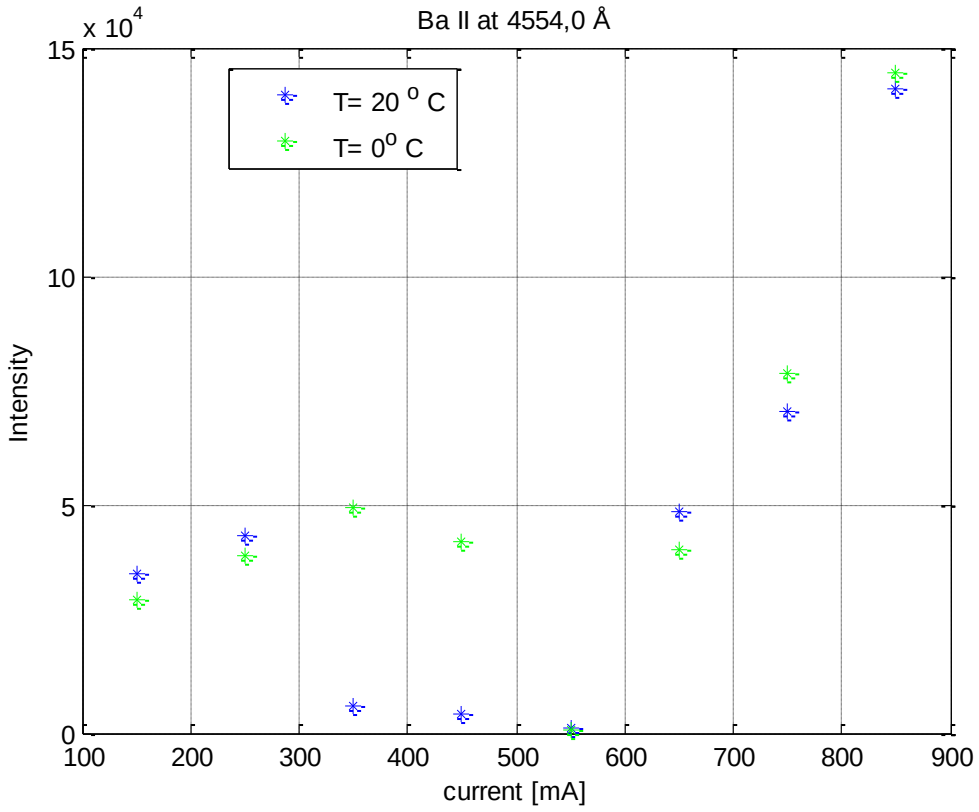

Figure 7.1 shows the dependence between intensity and current in Ba II 4554,0 Å at two different temperatures (T= 20 ° C and T=0 ° C).

The results from the Ba II measurements illustrate the fact that there is an optimum temperature/discharge current for the electrode. When the cathode is cold at low currents, the cathode fall is high and the phenomenon of sputtering (when free electrons hit the electrode so electrons leave the cathode) is most probable. At higher currents, the cathode will warm up trough resistive heating and the cathode fall will diminish. At even higher currents and electrode temperatures, evaporation of the cathode material will set in.

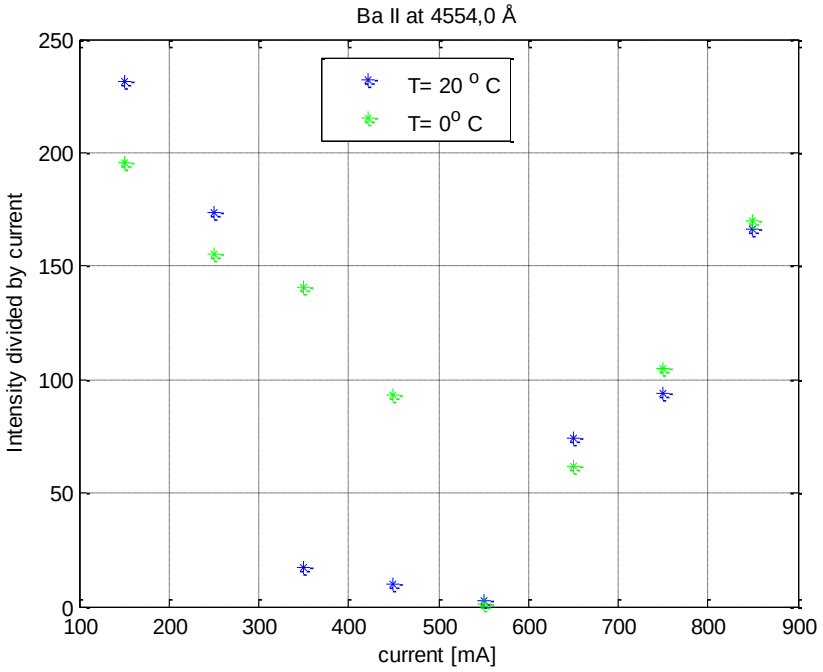

Figure 7.2 shows the dependence between intensity divided by current and current in Ba II 4554,0 Å at two different temperatures (T= 20 ° C and T=0 ° C).

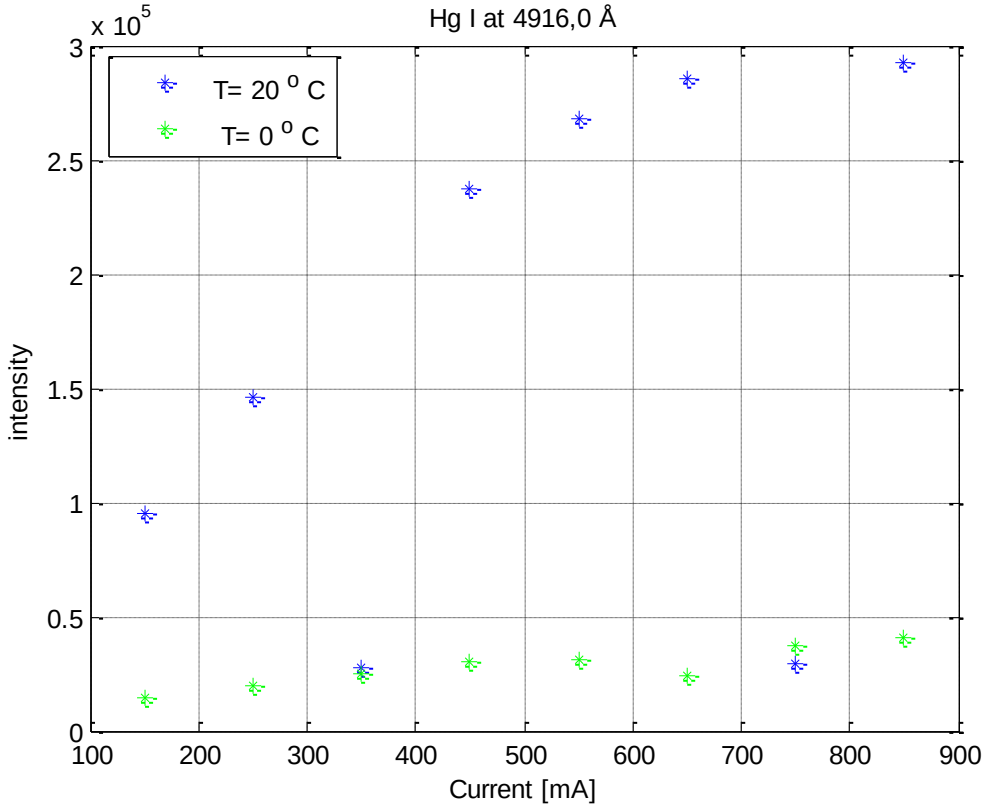

Figure 7.3 shows the dependence between intensity and current in Hg I 4916,0 Å at two different temperatures (T= 20 ° C and T=0 ° C).

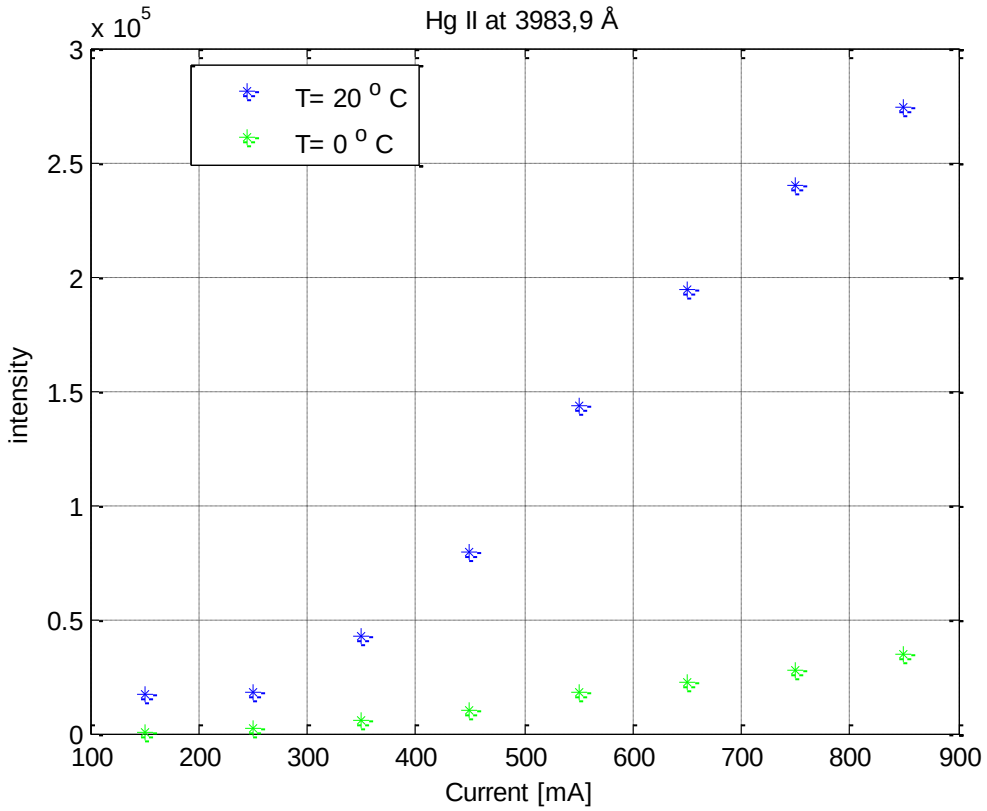

Figure 7.4 shows the dependence between intensity and current in Hg II 3983,9 Å at two different temperatures (T= 20 ° C and T=0 ° C).

There is a distinct difference between the results of Hg I and Hg II. In Hg I the upper level of the observed transition may be populated from direct electron collision.

$e^- + Hg \rightarrow Hg^* + e^-$

Where Hg, represents neutral Hg and Hg^* represents exited Hg.

The intensity rises linearly with the current until the time between electron collision approaches the lifetime of the excited level, when a kind of thermal equilibrium is reached.

In Hg II a quadratic current dependence is observed. Due to the high energy required to populate the upper level of the transition observed in Hg II relative to the ground state of Hg I, it is most probable that the excitation processes takes place in two or more steps and because of this it shows quadratic tendencies. This leads to population of the excited level being proportional to a higher power of the electron density or current, which indeed is observed in Hg II *see figure 7.3 and 7.4.*

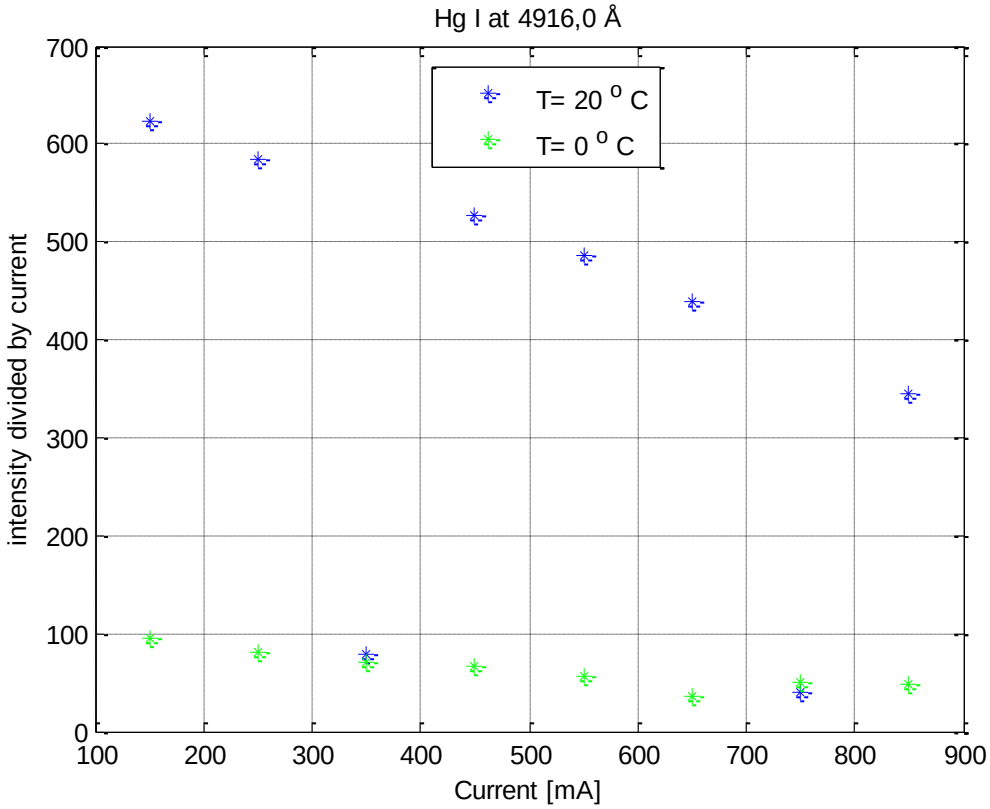

Figure 7.5 shows the dependence between intensity divided by current and current in Hg I 4916,0 Å at two different temperatures (T= 20 ° C and T=0 ° C).

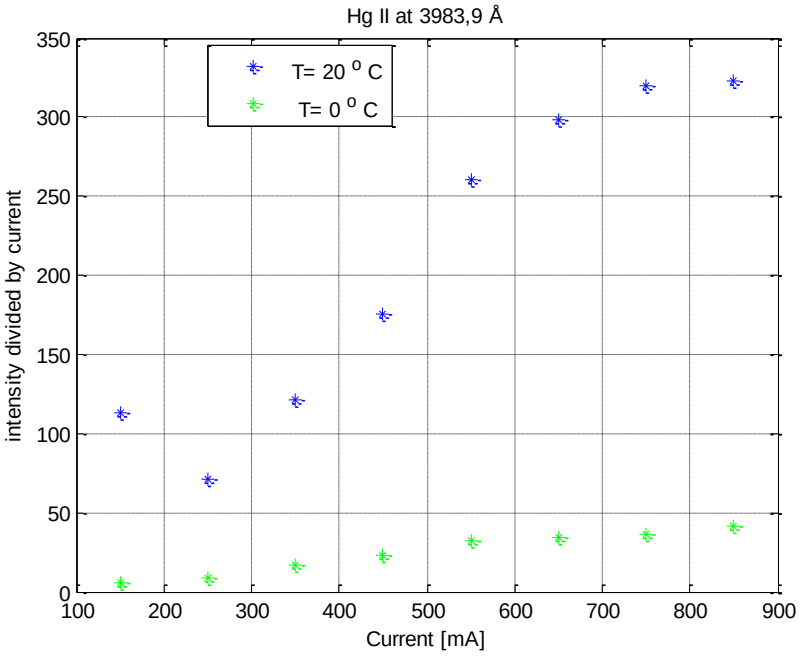

Figure 7.6 shows the dependence between intensity divided by current and current in Hg II 3983,9,9 Å at two different temperatures (T= 20 ° C and T=0 ° C).

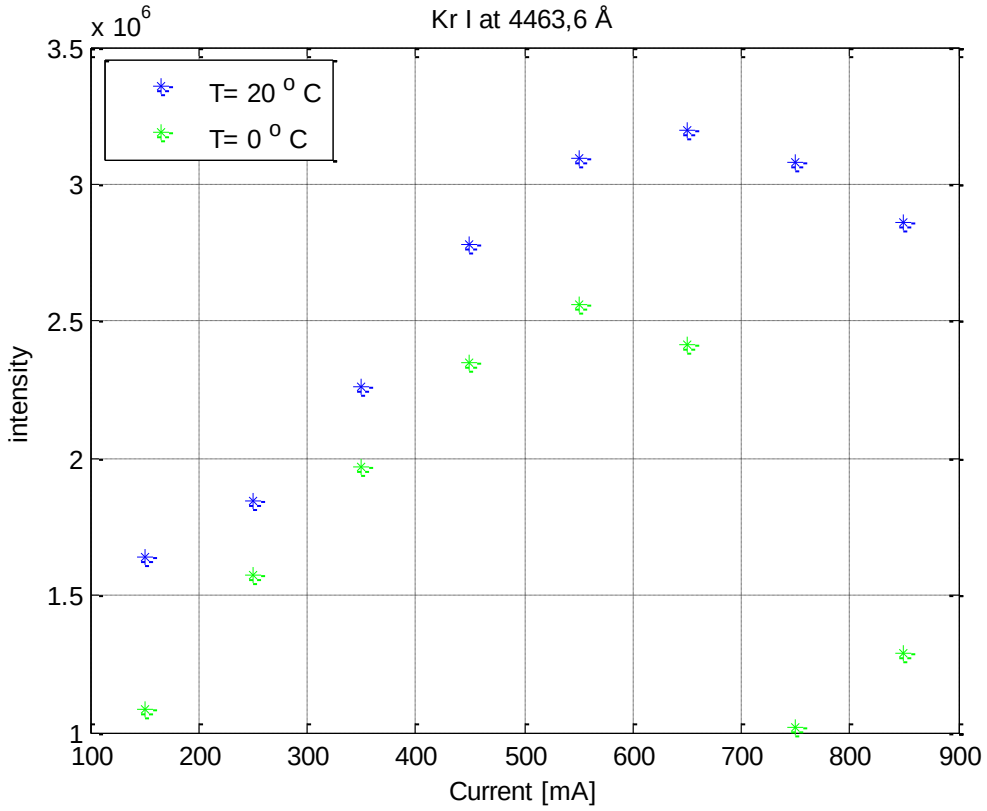

Figure 7.7 shows the dependence between intensity and current in Kr I 4463,6 Å at two different temperatures (T= 20 ° C and T=0 ° C).

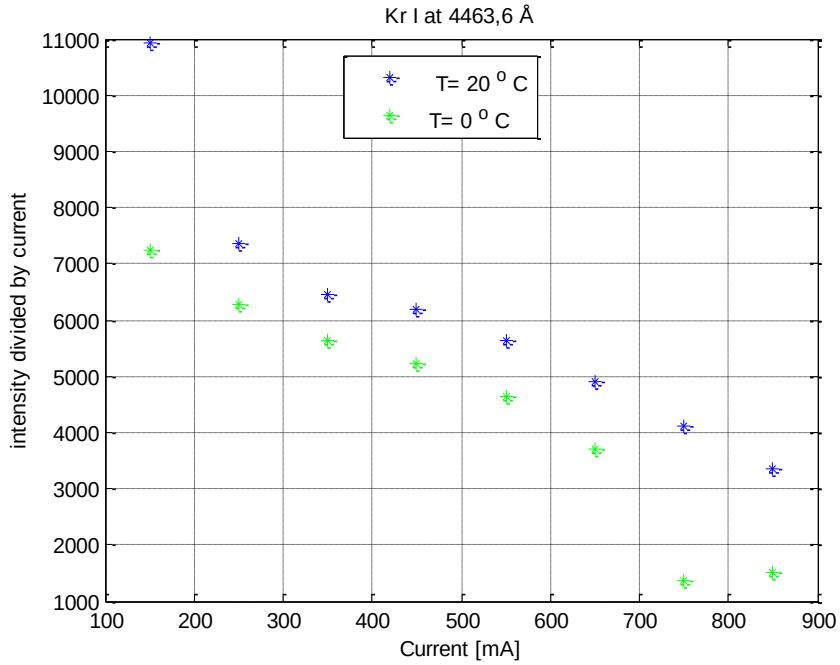

Figure 7.8 shows the dependence between intensity divided by current and current in Kr I 4463,6 Å at two different temperatures (T= 20 ° C and T=0 ° C).

7.1 Results from the time resolved measurements

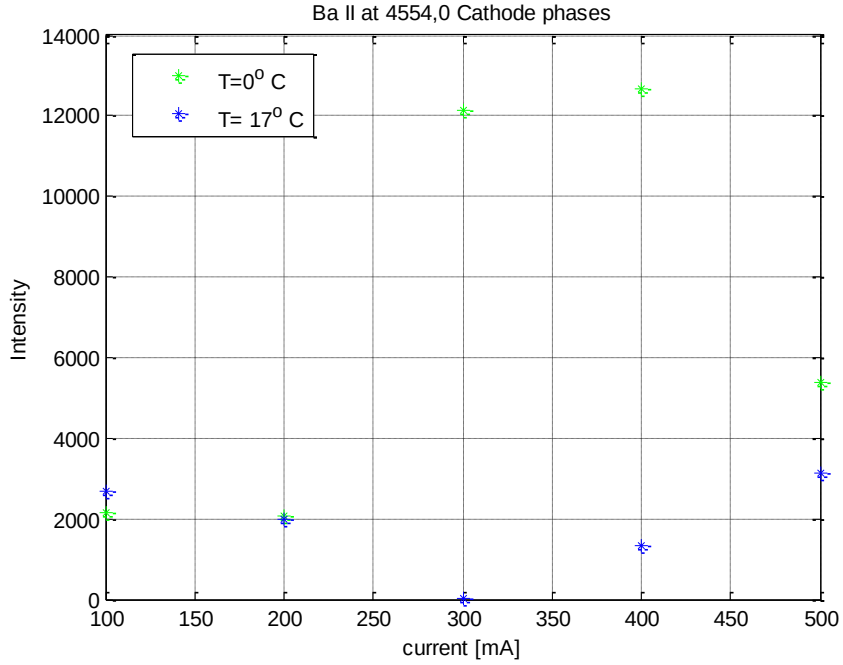

Figure 7.9 shows the dependence between intensity and current of the cathode phases in Ba II 4554,0 Å at two different temperatures.

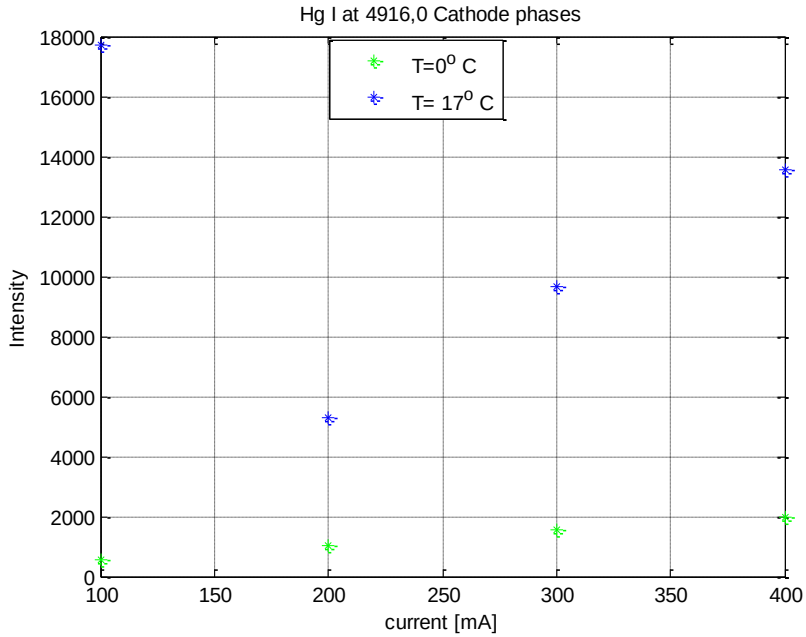

Figure 7.10 shows the dependence between intensity and current of the cathode phases in Hg I 4916,0 Å at two different temperatures.

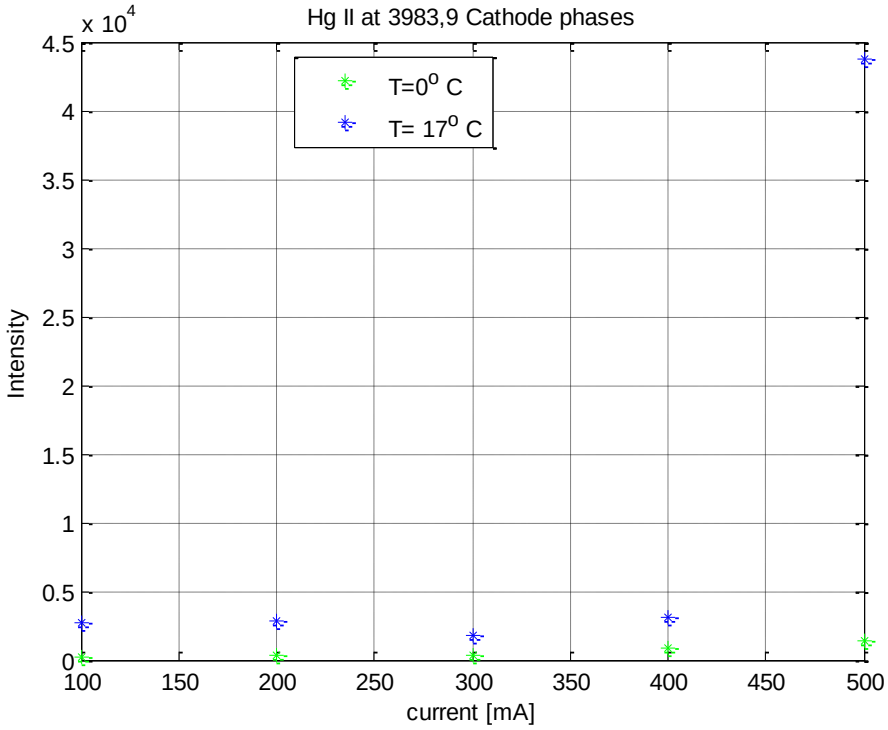

Figure 7.11 shows the dependence between intensity and current of the cathode phases in Hg II 3983,9 Å at two different temperatures.

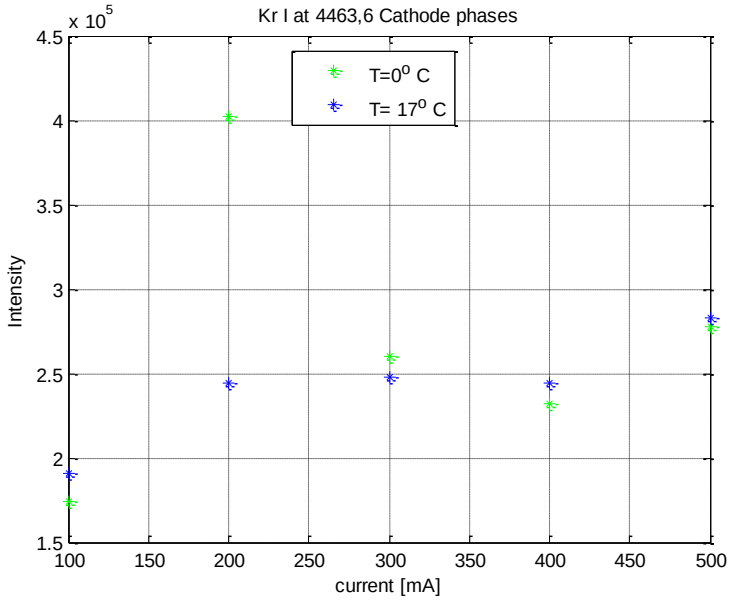

Figure 7.12 shows the dependence between intensity and current of the cathode phases in Kr I 4463,6 Å at two different temperatures.

8. Discussion

The time resolved measurements confirmed that most of the emissions take place during the cathode phase especially in mercury (Hg I and Hg II).
Fluctuations occurred mainly at low currents (100-350 mA), which may explain why some of the results show inconsistent tendencies at these currents.

From the performed measurements, it is possible to make limited conclusions about the excitation. Most of the energy levels in Hg I are probably populated by direct electron collision, which gives a linear dependence between intensity and current shown in *figure 7.3.* The relation between ionized mercury (Hg II) shows quadratic dependence *see figure 7.4,* which suggests that the excitation of the ($5d^9 6s^2$) level takes place in two or more-step processes in contrast to Hg I.
In Hg I the intensity rises in portion to the current until, high currents (550 mA-850mA) collisional deexcitation is starting to compete with spontaneous decay, indicating that a partial thermal equilibrium is reached.
The intensities of cooled (0 ^{o} C) Hg is much weaker (order of magnitude 10^3) than those preformed at 20 ^{o} C, (order of magnitude 10^4-10^5) because the amount of Hg changes with temperature. This is a great problem in cold places on earth.

Strong emission of barium atoms from the electrodes will occur if the electrodes are to warm or cold which is suggested by *figure 7.1* and *7.2.* This will wear the electrodes out, which is a great problem when dimming fluorescent light tubes. For this reason, additional external electrode heating must be supplied in order to keep the temperature of the electrode at sufficiently high temperature when the discharge currents are low.
The intensity of the rare gas emission rises in portion to the current until saturation effects will level out the dependence, as shown in *figure 7.7.*

The measurements themselves are not especially time consuming, but cooling the circulating water to 0 ^{o} C is very time consuming. When the water has been cooled, it is not possible to perform any measurements of room temperature in 24 hours.
The plasma will not be disturbed at all by using this method which is a great advantage. But processes which do not emit light will not be possible to observe.

9. Conclusions

This project was preformed to try to distinguish between different excitation possesses in low pressure plasmas, by using optical emission spectroscopy. Four spectral lines were investigated (Hg I 4916,0 Å, Hg II 3983,9 Å, Ba II 4554 ,0 Å, Kr I 4463,6 Å) with a Czerny-Turner spectrograph and an ICCD camera, as light source a T 18 W fluorescent light tube was used. If the exposure time is too long the ICCD camera might be saturated. If a spectral line is saturated it will not give any reasonable results. Sometimes it was hard to determine how short the exposure time should be, but it should not be shorter than tens of a second because the ICCD camera will not be effective for shutter times that short. On the other hand the

shutter time should not be longer than 20 seconds either. If the shutter time is longer, too much background will be introduced into the spectrum.
The used method gave reproducible results, and it was confirmed that most of the emission takes place during the cathode phase.

There is an optimal discharge current for the electrodes. When the current is low the electrode is cold and sputtering will occur due to the cathode fall. When the current is high the electrodes will be warm and vaporization of the electrode material (in this case barium) will occur. It is a great problem to keep the temperature of the electrode constant when dimming a fluorescent light tube. It was found that the excitation processes in mercury takes place in two or more-step processes, and that the energy levels most likely is populated by direct electron collision. In krypton the intensity rises in portion to the current until saturation, which was expected. It would be possible from the performed measurements to say something about which gas mixtures will occur.

10. Acknowledgements

I would like to thank my supervisor Sven Huldt and PhD. Student Thomas Lennartsson for making this thesis possible.
At last I want to thank my best friend Daniel Hägg for all your support in this thesis and in life.

11. References

[1] Waymouth, J.F., Electric Discharge Lamps, MIT, Cambridge, 1971.

[2] Introduction to plasma physics with space and laboratory applications by Donald A.Grunett and Amitava Bhattacharjee 2005.

[3] INSTRUCTION MANUAL model 78-460 SERIES and 78-490 SERIES 1C METER and 0.75 METER CZERNY-TURNER SCANNING SPRCTROMETER/SPECTROGRAPH. Engineering Pub. No. 78-460/IM , Rev. 1 June 1967

[4] Instruction Manual TCP202 15 Ampere AC/DC Current probe

[5] A spectroscopic investigation of the effect of electrode heating in fluorescent tube lamps Bachelor Thesis By Moah Christensen Fall 2008

[6] Time resolved Spectroscopy in low pressure plasmas
Master Thesis by Johannes Lindén June 2005

[7]Investigation of Excitation Processes in Laboratory Plasmas Using Time-resolved Spectroscopy
Master thesis by Joel Clementson July 2005

[8] spectrophysics principals and applications by A. Thorne U. Litzén S. Johansson, Lund 2007.

12. Appendix

12.1 A1 Matlab script

```
clear all
close all
sn ='HgII_150mA.asc'; % the loaded spectrum
CCDimage = load(sn);

lowLimit =480;  % limits of the wanted interval
highLimit =600;
t=20; % exposure time
slice = (1/t)*CCDimage(:,lowLimit:highLimit);
I = sum(slice,2);
figure(1)
plot(I)
title(sn);
 backgroundValue = 2800;
 left =395; % limits of the wanted interval
 right = 403;

Isummed = sum(I(left:right)-noiceValue) % integrates from left to right and
subtracts the noise
```